Bull. Health Sci. Hirosaki 4 : 83－91, 2005

Quasi-monochromatic fine polycapillary imaging utilizing computed radiography system

—— X-ray lens for biomedicine ——

Toshio ICHIMARU[*1], Eiichi SATO[*2], Etsuro TANAKA[*3]
Hidezo MORI[*4], Toshiaki KAWAI[*5], Sigehiro SATO[*6]
and Kazuyoshi TAKAYAMA[*7]

(Received October 31, 2004 ; Accepted January 13, 2005)

Abstract : A fundamental study on quasi-monochromatic radiography using a polycapillary plate and a copper-target x-ray tube is described. The tube voltage was regulated from 12 to 22 kV, and the tube current was regulated within 3.0 mA by the filament temperature. The exposure time was controlled in order to obtain optimum x-ray intensity, and the maximum focal spot dimensions were approximately 2.0 × 1.5 mm. The polycapillary plate was J5022-16 (Hamamatsu Photonics Inc.), and the plate thickness was 1.0 mm. The outer, effective, and hole diameters were 33 mm, 27 mm, and 10 μm, respectively. Quasi-monochromatic x rays were produced using a 10-μm-thick copper filter with a tube voltage of 17 kV, and these rays were formed into quasi-parallel beams by the polycapillary. The radiogram was taken using a computed radiography system utilizing imaging plates. The spatial resolution hardly varied according to increases in the distance between the spatial resolution-test chart and imaging plate using a polycapillary. We could observe a 50 μm tungsten wire, and fine blood vessels of approximately 100 μm were visible in angiography.

Key words : quasi-parallel radiography, quasi-monochromatic xrays, characteristic xrays, x-ray lens, polycapillary plate

1. INTRODUCTION

Monochromatic parallel x-ray beams are typically produced by a synchrotron in conjunction with single crystals and have been applied in high contrast micro-angiography[1] and x-ray phase imaging.[2－4] In order to produce quasi-monochromatic x rays without using the synchrotron, we developed a transmission type molybdenum x-ray tube.[5] Subsequently, flash x-ray tubes are employed to

*1 Department of Radiological Technology, School of Health Sciences, Hirosaki University, 66-1 Hon-cho, Hirosaki-shi, Aomori-ken 036-8564, Japan. E-mail: ichimaru@cc.hirosaki-u.ac.jp
*2 Department of Physics, Iwate Medical University, 3-16-1 Hon-cho-dori, Morioka-shi, Iwate-ken 020-0015, Japan.
*3 Department of Nutritional Science, Faculty of Applied Bio-science, Tokyo University of Agriculture, 1-1-1 Sakuragaoka, Setagaya-ku, Tokyo 156-8502, Japan.
*4 Department of Cardiac Physiology, National Cardiovascular Center Research Institute, 5-7-1 Fujishiro-dai, Suita-shi, Osaka 565-8565, Japan.
*5 Electron Tube Division, Hamamatsu Photonics K. K., 314-5 Shimokan-zo, Toyooka village, Iwata-gun, Shizuoka-ken, 438-0193, Japan.
*6 Department of Microbiology, School of Medicine, Iwate Medical University, 19-1 Uchimaru, Morioka-shi, Iwate-ken 020-8505, Japan.
*7 Shock Wave Research Center, Institute of Fluid Science, Tohoku University, 2-1-1 Katahira, Aoba-ku, Sendai-shi, Miyagi-ken 980-8577, Japan.

primarily perform high-speed radiographies with biomedical applications. In particular, plasma flash x-ray tubes are very useful to produce intense and sharp characteristic xrays[6-11] such as lasers.

With recent advances in x-ray optics, several different x-ray lenses[12,13] have been developed, and a polycapillary plate[5,8,14] has been shown to be useful to realize a low-priced x-ray system and to perform quasi-parallel radiography. Therefore, we performed polycapillary imaging using a tungsten-target x-ray tube and an x-ray film because the film is conventional and is useful to obtain a high image resolution.

In biomedical radiography, because both the brightness and the contrast of radiograms can be controlled by a Computed Radiography (CR) system[15] utilizing imaging plates, the CR system is useful to perform quasi-monochromatic polycapillary imaging, regardless of whether the image resolution falls.

In this article, we describe a quasi-monochromatic parallel radiography system utilizing a fine polycapillary plate with a hole diameter of 10 μm, a CR system, and a copper-target radiation tube in order to create a conventional x-ray system to be used instead of the synchrotron.

2. EXPERIMENTAL SETUP

Figure 1 shows the circuit diagram of the x-ray generator, which consists of a negative high-voltage power supply, a filament (hot cathode) power supply, and a copper-target x-ray tube. The negative high-voltage is applied to the cathode electrode, and the anode (target) is connected to the ground. In this experiment, the tube voltage was regulated from 12 to 22 kV, and the tube current was regulated by the filament temperature and ranged from 1.0 to 3.0 mA. The exposure time was controlled in order to obtain optimum x-ray intensity.

The experimental setup for performing quasi-parallel radiography is shown in Fig. 2. Quasi-monochromatic x rays are produced using a 10-μm-thick copper filter, and these rays are formed into quasi-parallel beams by a polycapillary plate (Fig. 3). The polycapillary is J5022-16 (Hamamatsu Photonics Inc.), and the thickness and the hole diameter of the polycapillary are 1.0 mm and 10 μm, respectively. Radiography

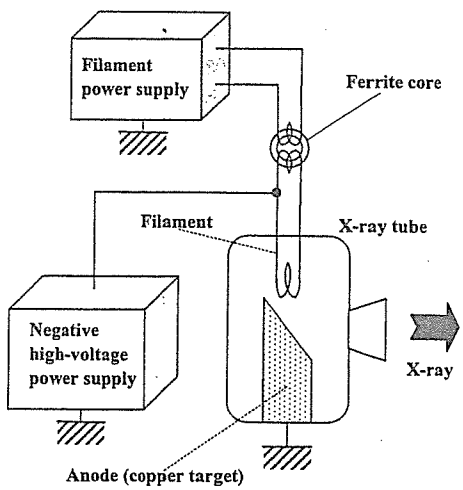

Fig. 1. Circuit diagram of the x-ray generator.

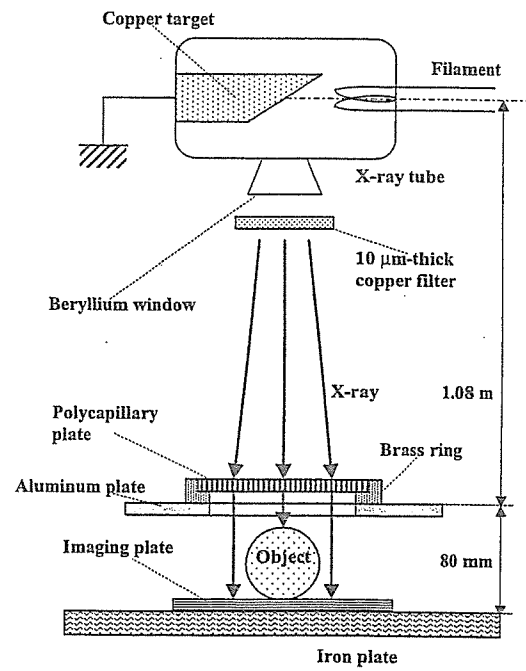

Fig. 2. Experimental setup for quasi-parallel radiography utilizing a polycapillary plate and a CR system.

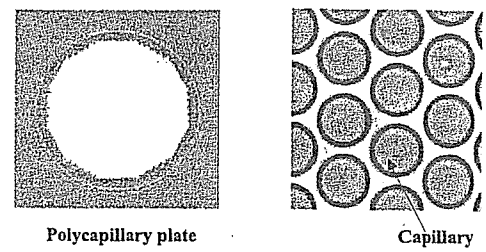

Fig. 3. Polycapillary plate.

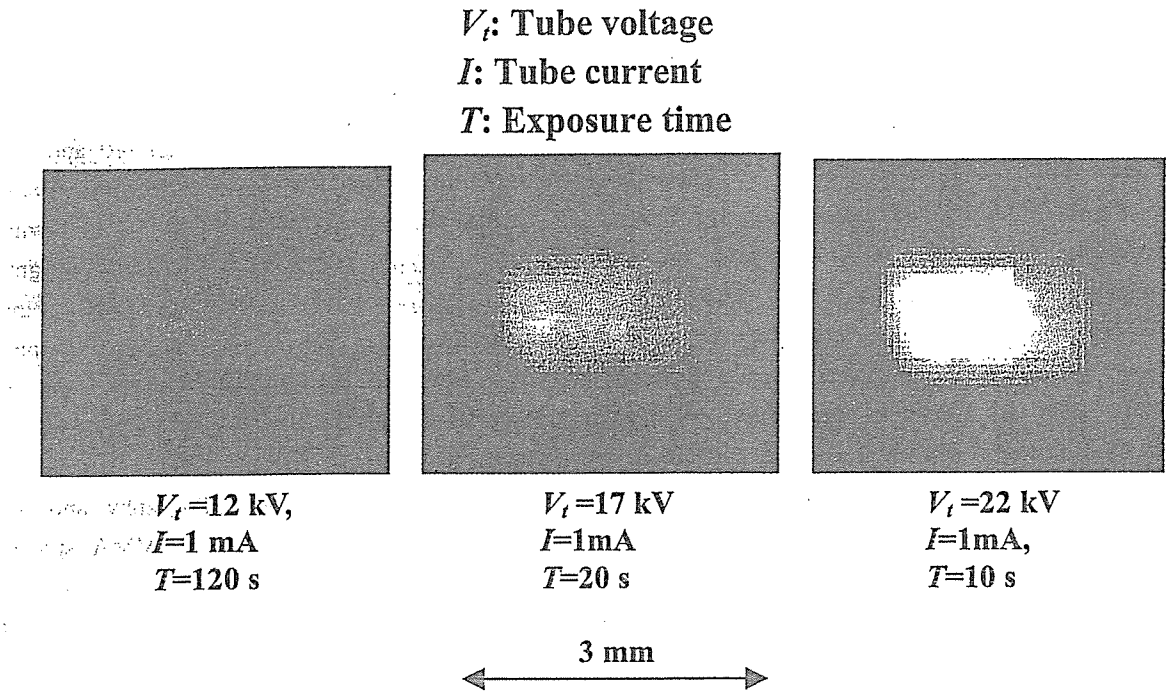

Fig. 4. Images of the x-ray source measured by a 50-μm-diameter pinhole with changes in the tube voltage.

was performed by a CR system (Konica Regius 150) utilizing imaging plates, and the distance between the x-ray source and the polycapillary was 1.08 m.

3. CHARACTERISTICS

3.1 *Focal Spot*

In order to measure images of the x-ray source, we employed a pinhole camera with a hole diameter of 50 μm (Fig. 4). When the tube voltage was increased, the spot intensity increased, and spot dimensions increased slightly and had values of approximately 2.0×1.5 mm.

3.2 *X-ray Spectra*

X-ray spectra from the copper-target tube were measured by a transmission-type spectrometer with a lithium fluoride curved crystal 0.5 mm in thickness. The spectra were taken by the CR system with a wide dynamic range, and relative x-ray intensity was calculated from DICOM (Digital Imaging and Communications in Medicine) digital data. Figure 5 shows measured spectra from the copper target. When the tube voltage was increased, the bremsstrahlung x-ray intensity increased, and the characteristic x-ray intensity of Kα and Kβ lines also increased. Following insertion of the copper filter, the bremsstrahlung x

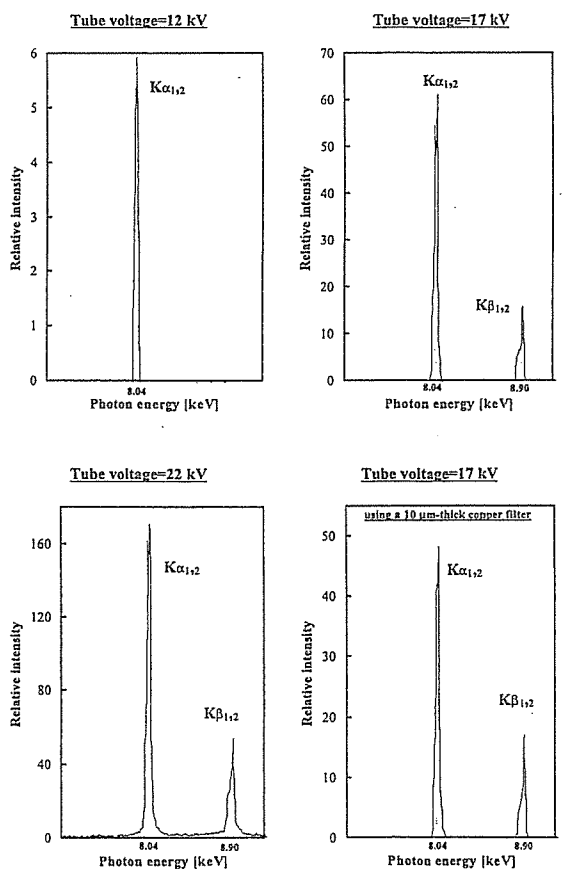

Fig. 5. Measured x-ray spectra according to changes in the tube voltage using a 10-μm-thick copper filter.

rays with energies higher than the K-absorption edge were absorbed effectively.

4. RADIOGRAPHY

The quasi-monochromatic radiography was performed with a tube voltage of 17 kV using the filter. Figure 6 shows radiography for imaging a polycapillary plate, and the radiograms of the polycapillary are shown in Fig. 7. The center of the black spot in the polycapillary radiogram was mainly imaged by direct transmission beams through capillary holes. As shown in this figure, the spot dimensions increased slightly according to decreases in the polymethyl methacrylate (PMMA) spacer height.

Figure 8 shows the polycapillary radiography for imaging a test chart, and the polycapillary was set on the brass ring. In this radiography, when the spacer height was increased, the image resolution hardly varied, and the image dimensions decreased slightly (Fig. 9). Enlarged radiograms of the test chart (166 μm lead lines) are shown in Figs. 10 and 11. When the polycapillary was employed, the image contrast of lines increased, but the resolution hardly varied. With increases in the brass spacer height, the image resolution hardly varied, and the dimensions again decreased slightly (Figs. 12 and 13). When the polycapillary was employed in conjunction with the brass spacer, the contrast again increased.

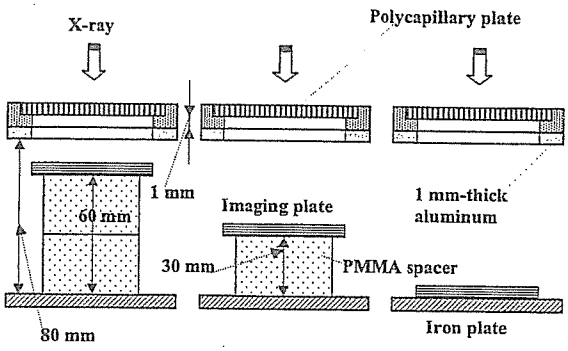

Fig. 6. Radiography for imaging a polycapillary plate according to changes in the distance between the polycapillary and imaging plates.

Figures 14 and 15 show radiography and the radiogram of tungsten wires on a PMMA spacer, respectively. Although the image contrast increased with increases in the wire diameter, a 50 μm-diameter wire could be observed. An angiography of a rabbit heart (coronary artery) is shown in Fig. 16; iodine-based microspheres of 15 μm diameter were used, and fine blood vessels of about 50 μm were visible (Fig. 17).

5. DISCUSSION

In this research, we performed quasi-parallel radiography achieved with a polycapillary plate in conjunction with quasi-monochromatic x rays, and obtained slightly higher image resolutions as compared with those obtained without using the plate.

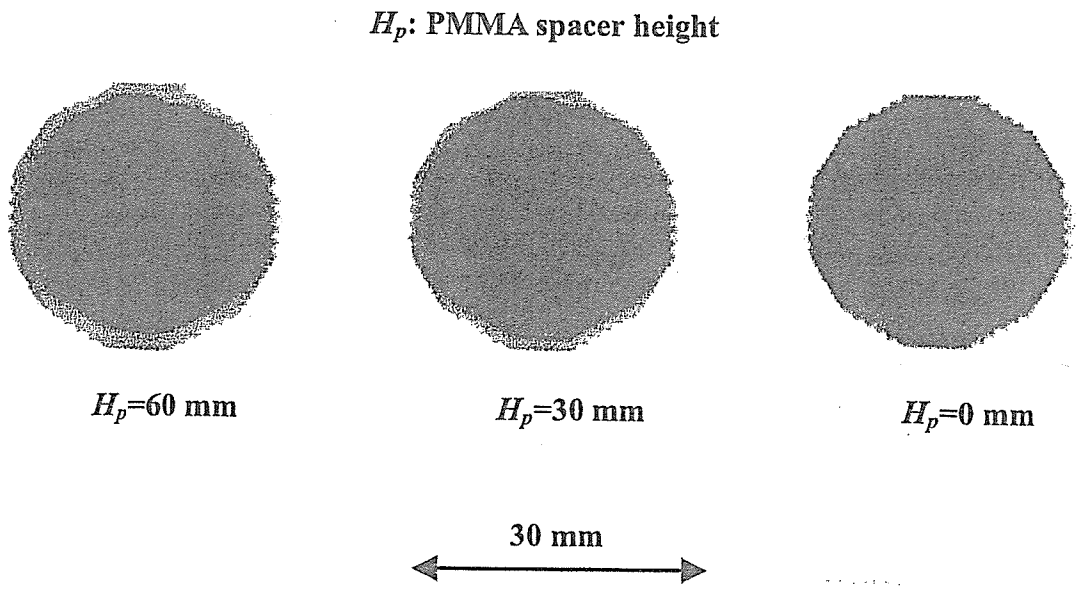

Fig. 7. Radiograms of a polycapillary plate according to changes in the PMMA height.

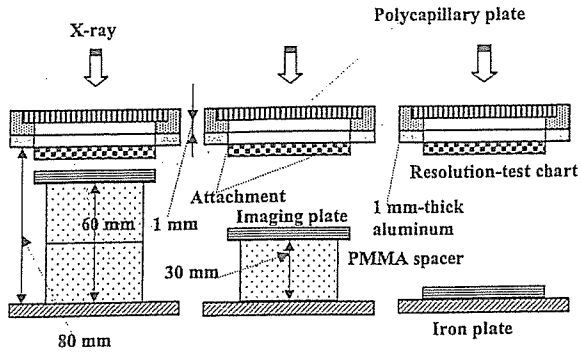

Fig. 8. Radiography for imaging a test chart using a polycapillary plate according to the PMMA height.

If we assume that the capillaries are completely straight, the image resolution of the polycapillary is primarily determined by the diameter of the capillary hole and the thickness, and is improved with decreases in the capillary diameter and increases in the thickness. In cases where the CR system is employed, although the resolution of the CR system is primarily determined by the minimum sampling pitch of 87.5 μm, we could observe 50 μm tungsten wires easily.

The photon energies of the characteristic x rays

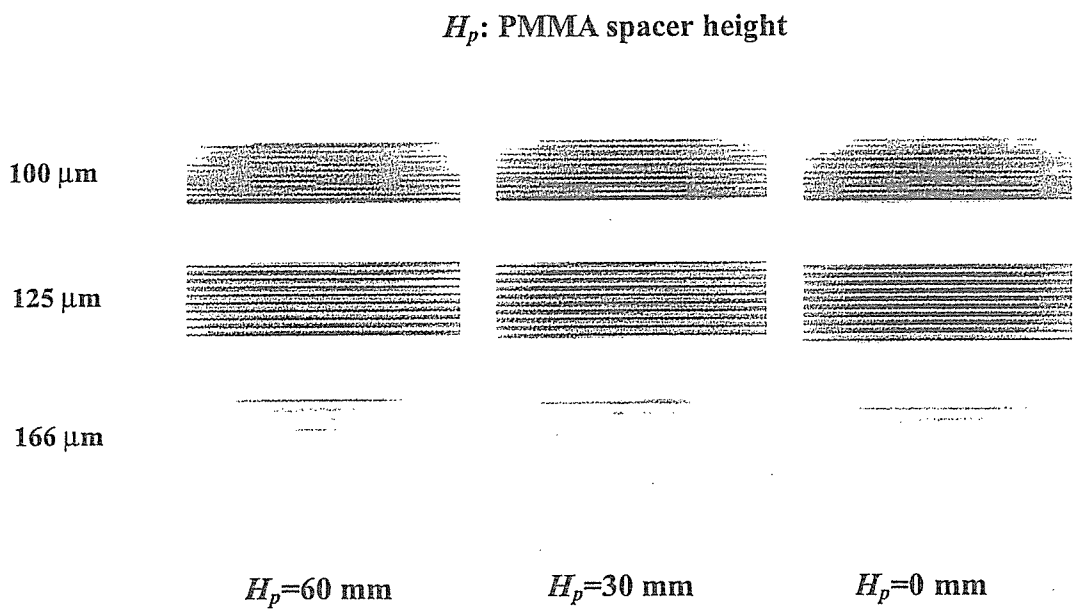

Fig. 9. Radiograms of a test chart using a polycapillary plate according to the PMMA height.

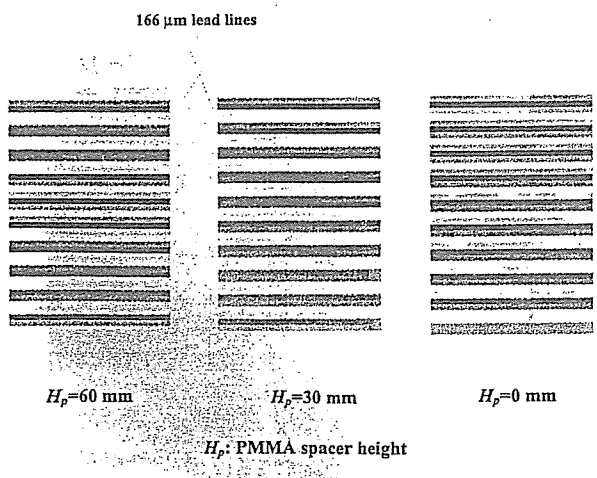

Fig. 10. Enlarged radiograms of a test chart using a polycapillary plate according to the PMMA height.

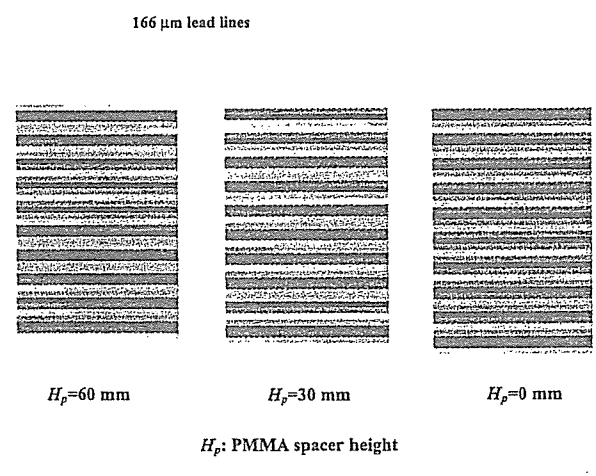

Fig. 11. Enlarged radiograms of a test chart without using a polycapillary plate according to the PMMA height.

are determined by the target element, and the capillary thickness should be increased according to increases in the photon energy because the transmission intensity through capillary glass increases. Subsequently, in order to increase the parallelity for phase imaging, single crystals should be employed after passing through the polycapillary.

Because it is possible to increase the irradiation field by increasing the distance between the x-ray source and the polycapillary, this system can be applied to image a wide variety of objects in various fields, including medical radiography.

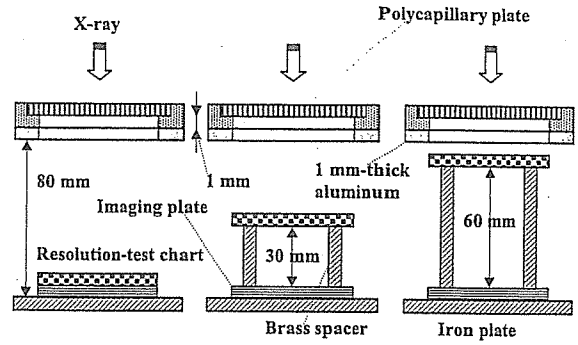

Fig. 12. Radiography for imaging a test chart using a polycapillary plate according to the brass spacer height.

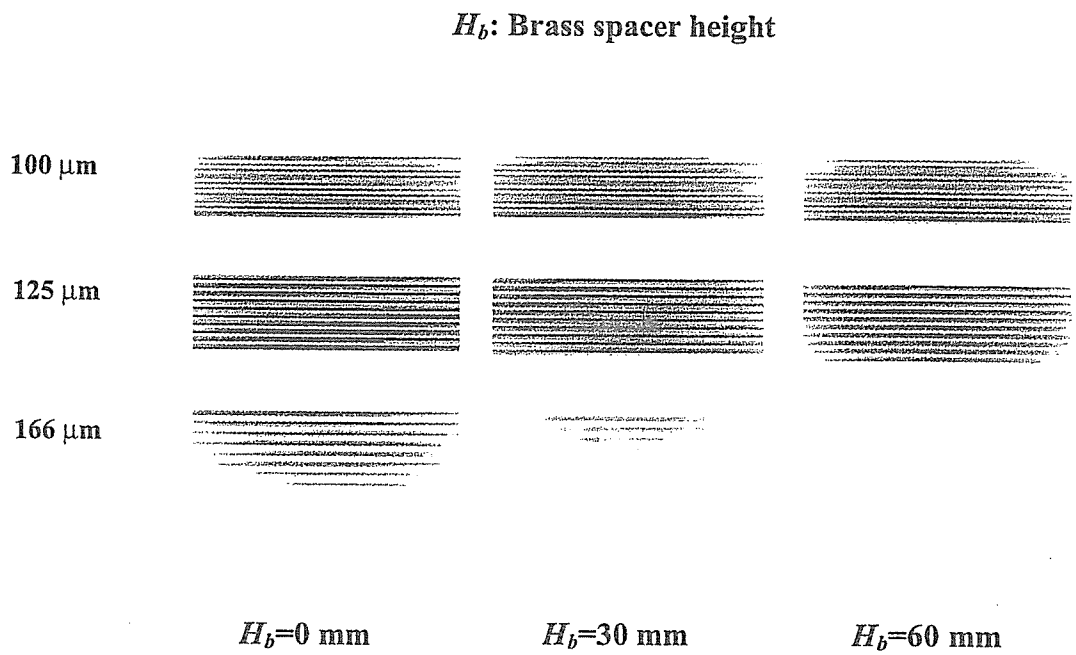

Fig. 13. Radiograms of a test chart using the polycapillary according to the brass spacer height.

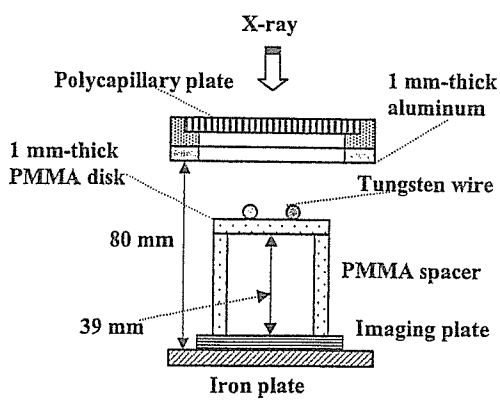

Fig. 14. Radiography for imaging tungsten wires using the polycapillary.

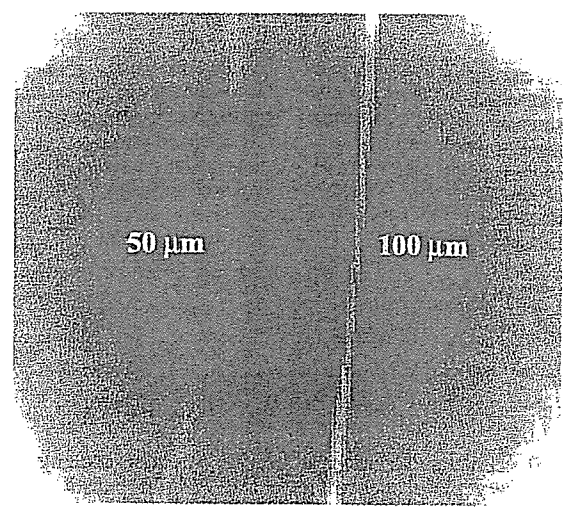

Fig. 15. Radiograms of tungsten wires on a PMMA spacer.

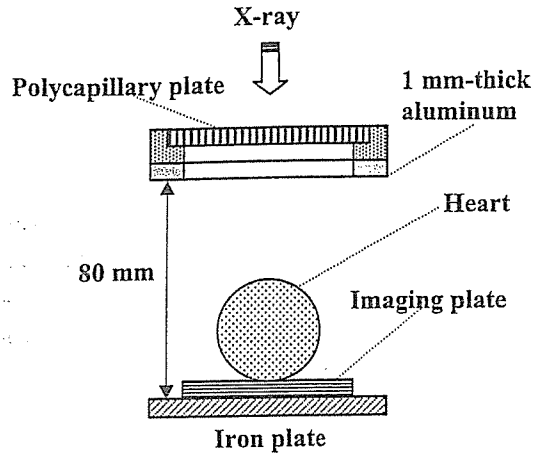

Fig. 16. Angiography of a heart extracted from a rabbit using iodine-based microspheres.

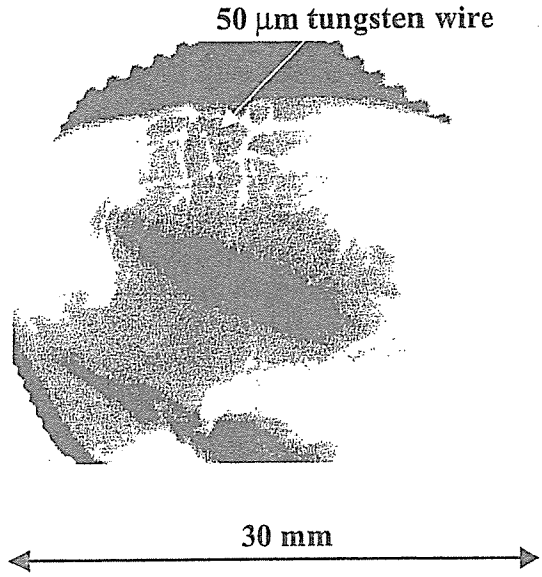

Fig. 17. Angiogram of the heart using the polycapillary.

ACKNOWLEDGMENTS

This work was supported by Grants-in-Aid for Scientific Research (13470154, 13877114, and 16591222) and Advanced Medical Scientific Research from MECSST, Health and Labor Sciences Research Grants(RAMT-nano-001, RHGTEFB-genome-005 and RHGTEFB-saisei-003), Grants from Keiryo Research Foundation, The Promotion and Mutual Aid Corporation for Private Schools of Japan, Japan Science and Technology Agency (JST), and New Energy and Industrial Technology Development Organization (NEDO, Industrial Technology Research Grant Program in '03).

REFERENCES

1) Mori H, Hyodo K, Tanaka E, Mohammed MU, Yamakawa A, Shinozaki Y, Nakazawa H, Tanaka Y, Sekka T, Iwata Y, Honda S, Umetani K, Ueki H, Yokoyama T, Tanioka K, Kubota M, Hosaka H, Ishizawa N and Ando M: Small-vessel radiography in situ with monochromatic synchrotoron radiation. *Radiology*, 201:173-177, 1996.
2) Davis TJ, Gao D, Gureyev TE, Stevenson AW and Wilkims SW: Phase-contrast imagimg of weakly absorbing materials using hard x-rays. *Nature*, 373: 595-597, 1995.
3) Momose A, Takeda T, Itai Y and Hirano K: Phase-contrast x-ray computed tomography for observing biological soft tissues. *Nature Medicine*, 2:473-475, 1996.
4) Ishisaka A, Ohara H and Honda C: A new method of analyzing edge effect in phase contrast imaging with incoherent x-rays. *Opt Rev*, 7:566-572, 2000.
5) Sato E, Komatsu M, Hayasi Y, Tanaka E, Mori H, Kawai T, Usuki T, Sato K, Ichimaru T, Takayama K and Ido H: Quasi-monochromatic parallel radiography achieved with a plane-focus x-ray tube. *Proc SPIE*, 4786:151-161, 2002.
6) Sato E, Hayasi Y, Mori H, Tanaka E, Takayama K, Ido H, Sakamaki K and Tamakawa Y: Quasi-monochromatic x-ray production from the cerium target. *Proc SPIE*, 4142:17-28, 2000.
7) Sato E, Suzuki Y, Hayasi Y, Tanaka E, Mori H, Kawai T, Takayama K, Ido H and Tamakawa Y: High-intensity quasi-monochromatic x-ray irradiation from the linear plasma target. *Proc SPIE*, 4505: 154-164, 2001.
8) Sato E, Hayasi Y, Tanaka E, Mori H, Kawai T, Obara H, Ichimaru T, Takayama K, Ido H, Usuki T, Sato K and Tamakawa Y: Polycapillary radiography using a quasi-x-ray laser generator. *Proc SPIE*, 4508:176-187, 2001.
9) Sato E, Hayasi Y, Tanaka E, Mori H, Kawai T, Usuki T, Sato K, Obara H, Ichimaru T, Takayama K, Ido H and Tamakawa Y: Quasi-monochromatic radiography using a high-intensity quasi-x-ray laser generator. *Proc SPIE*, 4682:538-548, 2002.
10) Sato E, Hayasi Y, Germer R, Tanaka E, Mori H, Kawai T, Obara H, Ichimaru T, Takayama K and Ido H: Irradiation of intense characteristic x-rays

from weakly ionized linear molybdenum plasma. *Jpn J Med Phys*, 20:123-131, 2003.

11) Sato E, Hayasi Y, Germer R, Tanaka E, Mori H, Kawai T, Obara H, Ichimaru T, Takayama K and Ido H: Intense characteristic x-ray irradiation from weakly ionized linear plasma and applications. *Jpn J Med Imag Inform Sci*, 20:148-155, 2003.

12) Xiao OF and Poturaef SV: Polycapillary-based x-ray optics. *Nucl Instr Meth Phys Res A*, 347:376-383, 1994.

13) MacDonald CA, Mail N, Li D, Roy M and Sugiro : Monochromatic applications of polycapillary optics. *Proc SPIE*, 5196:405-411, 2002.

14) Sato E, Toriyabe H, Hayasi Y, Tanaka E, Mori H, Kawai T, Usuki T, Sato K, Obara H, Ichimaru T, Takayama K, Ido H and Tamakawa Y: Fundamental study on parallel beam radiography using a polycapillary plate. *Proc SPIE*, 4682:298-310, 2002.

15) Sato E, Sato K and Tamakawa Y: Film-less computed radiography system for high-speed Imaging. *Ann Rep Iwate Med Univ Sch Lib Arts and Sci*, 35:13-23, 2000.

デジタルX線撮影システムを利用した準単色ファインポリキャピラリーイメージング
——医用X線レンズ——

市丸俊夫[*1] 佐藤英一[*2] 田中越郎[*3]
盛英三[*4] 河合敏明[*5] 佐藤成大[*6]
高山和喜[*7]

(2004年10月31日受付，2005年1月13日受理)

要旨：ポリキャピラリープレートと銅対陰極付きX線管を用いた準単色X線撮影に関して記述した。管電圧は12から22 kVの範囲で調整され，管電流はフィラメントの温度により3.0 mA以下に調整された。X線照射時間は撮影に適正なX線強度が得られるように制御され，実効焦点サイズは2.0×1.5 mmであった。ポリキャピラリープレートは浜松ホトニクス社製のJ5022-16でプレート厚は1.0 mmであった。外径，有効径，そして孔径はそれぞれ33 mm，27 mm，10 μmであった。管電圧が17 kVの条件下で銅のK系列特性（準単色）X線は，厚さ10 μmの銅フィルターを透して出力され，これらのX線はポリキャピラリーにより準平行化された。X線像はイメージングプレート付きのデジタル撮影システム（CR）により撮影された。空間分解能はテストチャートとプレート間の距離を増しても変化しなかった。撮影では50 μmのタングステンワイヤーが認識され，造影では100 μm程度の微小血管が観察できた。

キーワード：準平行X線撮影，準単色X線，特性X線，X線レンズ，ポリキャピラリープレート

*1弘前大学医学部保健学科放射線技術科学専攻
〒036-8565 青森県弘前市本町66番地1
E-mail: ichimaru@cc.hirosaki-u.ac.jp
*2岩手医科大学教養部物理学科
〒020-0015 岩手県盛岡市本町通3-16-1
*3東京農業大学応用生物科学部栄養科学科
〒020-0015 東京都世田谷区桜ヶ丘1-1-1
*4国立循環器センター研究所心臓生理部
〒565-8565 大阪府吹田市藤白台5-7-1
*5浜松ホトニクス電子管事業部
〒438-0193 静岡県磐田郡豊岡村下神増314-5
*6岩手医科大学医学部細菌学講座
〒020-0015 岩手県盛岡市内丸19-1
*7東北大学流体力学研究所
〒980-8577 宮城県仙台市青葉区片平2-1-1

Bull. Health Sci. Hirosaki 4 : 93—100, 2005

Cone-beam K-edge angiography utilizing cerium x-ray generator in conjunction with cerium oxide filter
—— Observation of fine blood vessels ——

Toshio ICHIMARU[*1], Akira YAMADERA[*1], Eiichi SATO[*2]
Etsuro TANAKA[*3], Hidezo MORI[*4], Toshiaki KAWAI[*5]
Sigehiro SATO[*6] and Kazuyoshi TAKAYAMA[*7]

(Received October 30, 2004 ; Accepted January 13, 2005)

Abstract : The cerium x-ray generator is useful in order to perform cone-beam K-edge angiography because K-series characteristic x rays from the cerium target are absorbed effectively by iodine-based contrast mediums. The x-ray generator consists of a main controller and a unit with a high-voltage circuit and a fixed anode x-ray tube. The tube is a glass-enclosed diode with a cerium target and a 0.5 mm-thick beryllium window. The maximum tube voltage and current were 65 kV and 0.4 mA, respectively, and the focal-spot sizes were 1.2 × 0.8 mm. Cerium K-series characteristic x rays were left using a cerium oxide filter, and the x-ray intensity was 0.50 μC/kg•s at 1.0 m from the source with a tube voltage of 60 kV, a current of 0.40 mA, and an exposure time of 1.0 s. Angiography was performed with a computed radiography system using iodine-based microspheres 15 μm in diameter. In angiography of non-living animals, we observed fine blood vessels of approximately 100 μm with high contrasts.

Key words : x-ray generator, cerium target, quasi-monochromatic x rays, characteristic x rays, K-edge angiography

1. INTRODUCTION

Monochromatic parallel x-ray beams are the basis of radiography using synchrotrons in conjunction with single crystals, and these beams have been employed to perform enhanced K-edge angiography [1-3] and x-ray phase imaging.[4-6] In angiography, the beams with photon energies of approximately 35 keV are absorbed effectively by iodine-based contrast mediums. However, it is difficult to obtain sufficient machine times for various research projects, including medical applications. Subsequently, monochromatic cone beams with energies of approximately 35 keV are useful in order to increase the irradiation field

*1 Department of Radiological Technology, School of Health Sciences, Hirosaki University, 66-1 Hon-cho, Hirosaki-shi, Aomori-ken 036-8564, Japan.
*2 Department of Physics, Iwate Medical University, 3-16-1 Hon-cho-dori, Morioka-shi, Iwate-ken, 020-0015, Japan.
*3 Department of Nutritional Science, Faculty of Applied Bio-science, Tokyo University of Agriculture, 1-1-1 Sakuragaoka, Setagaya-ku, Tokyo 156-8502, Japan.
*4 Department of Cardiac Physiology, National Cardiovascular Center Research Institute, 5-7-1 Fujishiro-dai, Suita-shi, Osaka 565-8565, Japan.
*5 Electron Tube Division, Hamamatsu Photonics K. K., 314-5 Shimokan-zo,Toyooka village, Iwata-gun, Shizuoka-ken, 438-0193, Japan.
*6 Department of Microbiology, School of Medicine, Iwate Medical University, 19-1 Uchimaru, Morioka-shi, Iwate-ken 020-8505, Japan.
*7 Shock Wave Research Center, Institute of Fluid Science, Tohoku University, 2-1-1 Katahira, Aoba-ku, Sendai-shi, Miyagi-ken 980-8577, Japan.

for K-edge angiography.

In order to perform high-speed medical radiography, although several different flash x-ray generators[7-13] utilizing cold-cathode tubes have been developed, plasma flash x-ray generators[14-18] are useful to produce quasi-monochromatic x rays without using a K-edge filter. Therefore, we have performed a demonstration of cone-beam K-edge angiography[19] utilizing a cerium plasma generator, since K-series characteristic x rays from the cerium target are absorbed effectively by iodine.

Recently, we have developed a steady state x-ray generator utilizing a cerium-target tube, and have demonstrated enhanced K-edge angiography utilizing a barium sulfate filter.[20] In this research, $K\alpha$ lines (34.6 keV) were left by absorbing $K\beta$ lines (39.2 keV), and bremsstrahlung x rays with photon energies of lower than the barium K-edge (37.4 keV) were also observed. However, because cerium $K\beta$ lines are also absorbed effectively by iodine, both $K\alpha$ and $K\beta$ lines should be selected to perform angiography. In measurements of x-ray spectra, although we usually employed a cadmium tellurium detector with a photon energy resolution of 1.7 keV, the resolution should be improved as much as possible to measure the characteristic x-ray intensity.

In the present research, we measured the x-ray spectra from a cerium-target tube using a germanium detector, and performed a preliminary study on cone-beam K-edge angiography achieved with cerium characteristic x rays using a cerium oxide K-edge filter.

2. GENERATOR

Figure 1 shows the block diagram of the x-ray generator, which consists of a main controller and an x-ray tube unit with a Cockcroft-Walton circuit and a cerium-target tube. The tube voltage, the current, and the exposure time can be controlled by the controller. The main circuit for producing x rays is illustrated in Fig. 2, and employed the Cockcroft-Walton circuit in order to decrease the dimensions of the tube unit. In the x-ray tube, the negative high voltage is applied to the cathode electrode, and the anode (target) is connected to the tube unit case (ground potential) to cool the anode and the target effectively. The filament heating current is supplied by an AC power supply in the controller in conjunction with an insulation transformer. The x-ray tube is a glass-enclosed diode with a cerium target and a 0.5-mm-thick beryllium window. In this experiment, the tube voltage applied was from 45 to 65 kV, and the tube current was regulated to within 0.40 mA (maximum current) by the filament temperature. The exposure time is controlled in order to obtain optimum x-ray intensity. Quasi-monochromatic x rays are produced using a cerium oxide filter for absorbing bremsstrahlung rays.

In designing the filter, the surface density of the cerium oxide powder is important, since the x rays are absorbed effectively by the powder as compared

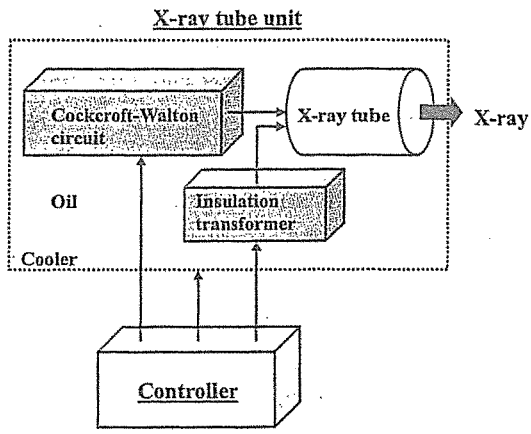

Fig. 1. Block diagram of compact x-ray generator with cerium-target radiation tube, which is used specially for K-edge angiography using iodine-based contrast mediums.

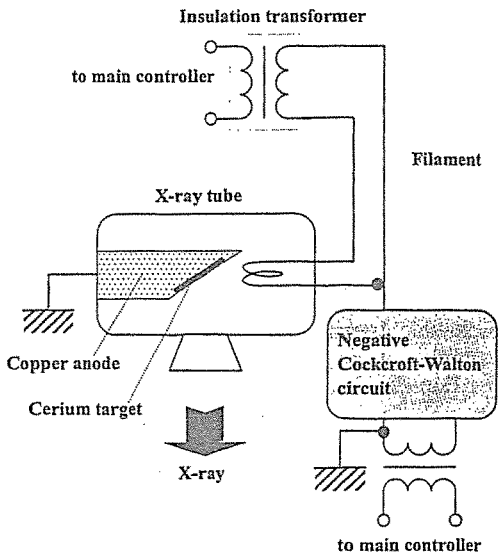

Fig. 2. Main circuit of x-ray generator.

with the PMMA powder. In this case, the density was approximately 10 mg/cm², and a K-edge powder filter (Fig. 3), consisting of cerium oxide and PMMA powders, was employed.

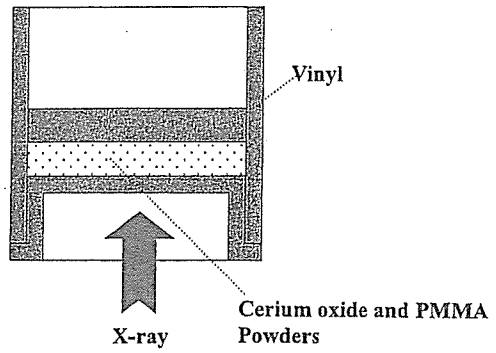

Fig. 3. Schematic drawing of cerium oxide powder filter.

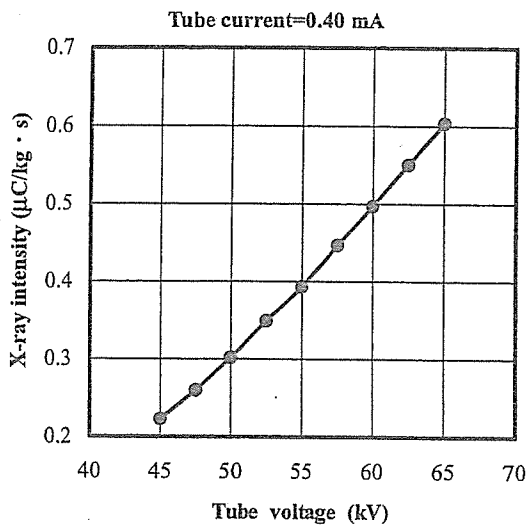

Fig. 4. X-ray intensity measured at 1.0 m from x-ray source according to changes in tube voltage.

3. CHARACTERISTICS

3.1 X-ray Intensity

X-ray intensity was measured by a Victoreen 660 ionization chamber at 1.0 m from the x-ray source using the filter (Fig. 4). At a constant tube current of 0.40 mA, the x-ray intensity increased when the tube voltage was increased. In this measurement, the intensity with a tube voltage of 60 kV and a current of 0.40 mA was 0.50 μC/kg·s at 1.0 m from the source with errors of less than 0.2%.

3.2 Focal Spot

In order to measure images of the x-ray source after the filtration, we employed a pinhole camera with a hole diameter of 50 μm (magnification ratio of 1:2) in conjunction with a Computed Radiography (CR) system[21] with a sampling pitch of 87.5 μm. When the tube voltage was increased, spot dimensions increased slightly and had values of 1.2 ×0.8 mm (Fig. 5).

3.3 X-ray Spectra

In order to measure x-ray spectra, we employed a germanium detector (GLP-10180/07-P, Ortec Inc.) with a photon energy resolution of approximately 0.12 keV (Fig. 6). When the tube voltage was increased, the characteristic x-ray intensities of Kα and Kβ lines substantially increased, and both the maximum photon energy and the intensities of bremsstrahlung x rays increased.

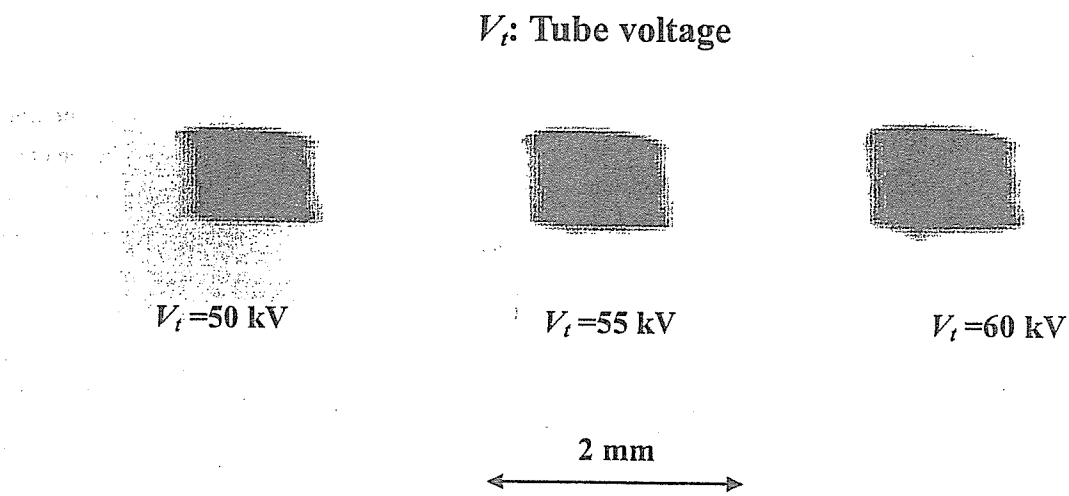

Fig. 5. Effective focal spots with changes in tube voltage.

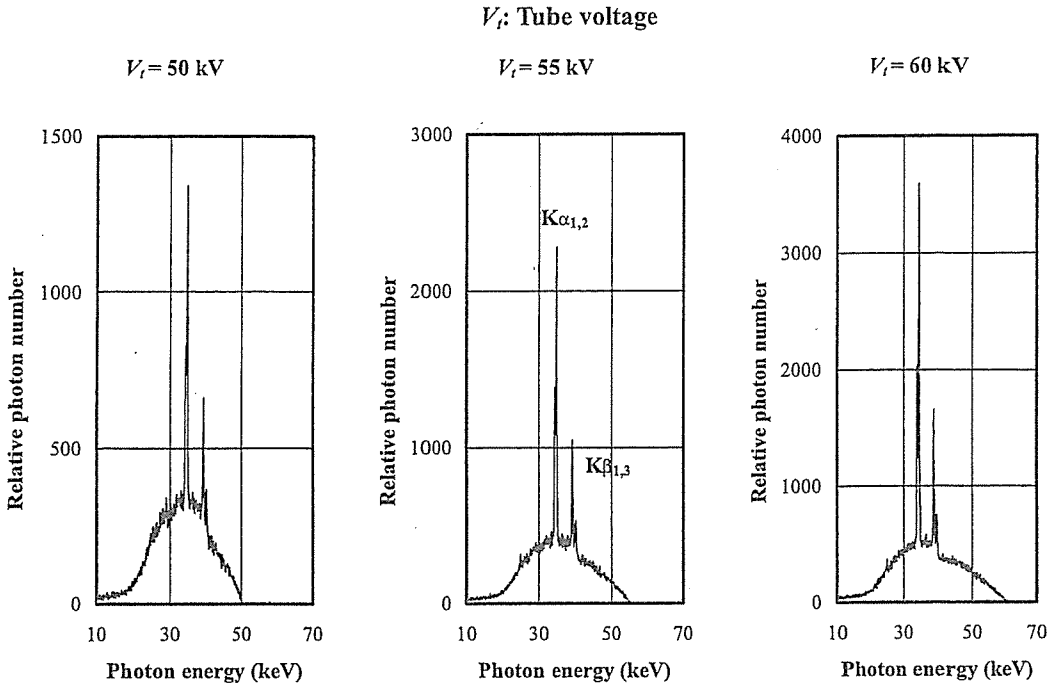

Fig. 6. X-ray spectra measured using germanium detector with changes in tube voltage.

4. K-EDGE ANGIOGRAPHY

Figure 7 shows the mass attenuation coefficients of iodine at the selected energies; the coefficient curve is discontinuous at the iodine K-edge. The average photon energy of the cerium Kα and Kβ lines are shown just above the iodine K-edge. Cerium is a rare earth element and has a high reactivity; however, the average photon energies of Kα and Kβ lines are 34.6 and 39.2 keV, respectively, and iodine contrast mediums with a K-absorption edge of 33.2 keV absorb the lines easily. Therefore, blood vessels were observed with high contrasts.

The angiography was performed by the CR system (Konica Regius 150) using the filter, and the tube voltage and the distance (between the x-ray source and the imaging plate) were 60 kV and 1.5 m, respectively. Firstly, rough measurements of spatial resolution were made using wires. Figure 8 shows radiograms of tungsten wires coiled around a rod made of polymethyl methacrylate. Although the image contrast decreased somewhat with decreases in the wire diameter, due to blurring of the image caused by the sampling pitch of 87.5 μm, a 50 μm-diameter wire could be observed.

Angiograms of rabbit hearts are shown in Fig. 9. These two images were obtained using iodine and cerium microspheres of 15 μm in diameter. In the case where the cerium spheres were employed, the coronary arteries were barely visible. Figures 10 and 11 show angiograms of a larger dog heart and a rabbit thigh, respectively, using iodine spheres. In angiography, the coronary arteries were visible, and fine blood vessels of approximately 100 μm could be seen.

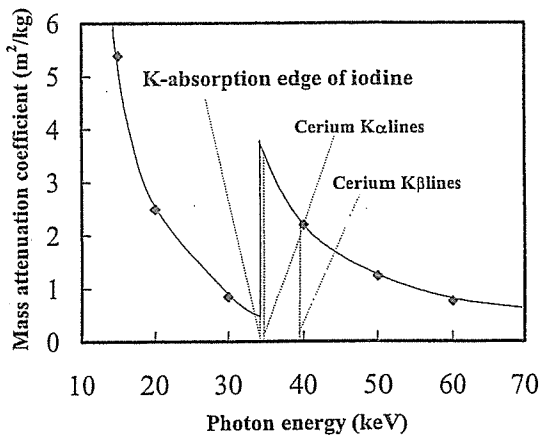

Fig.7. Mass attenuation coefficients of iodine, and average photon energies of cerium Kα and Kβ lines.

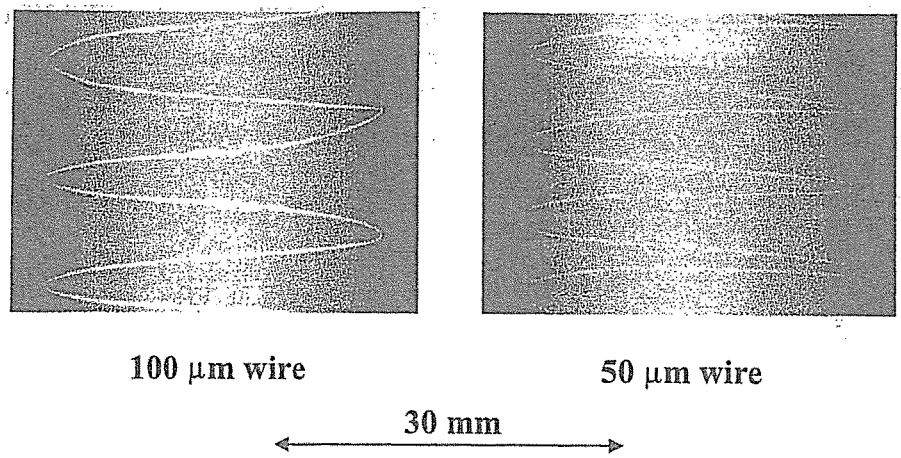

Fig. 8. Radiograms of tungsten wires in PMMA rod with tube voltage of 60 kV.

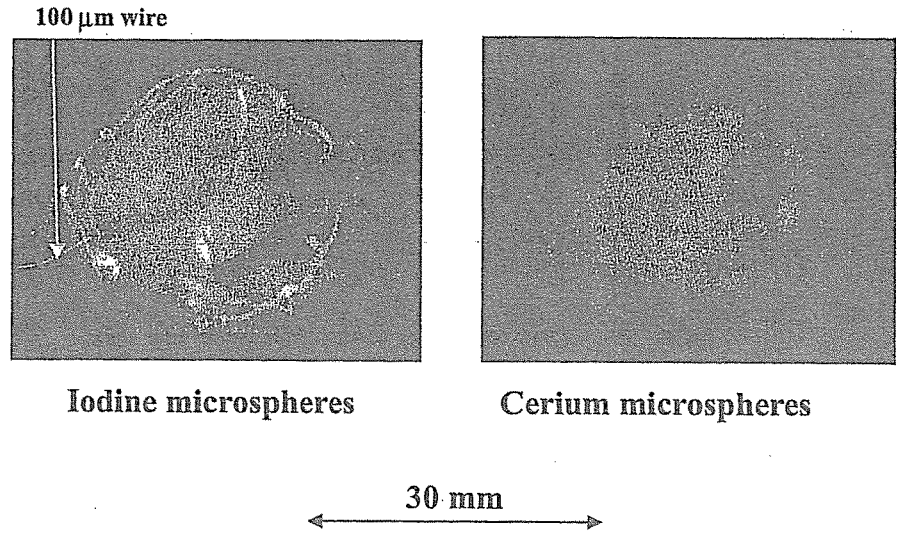

Fig. 9. Angiograms of extracted rabbit hearts using iodine and cerium microspheres with tube voltage of 60 kV.

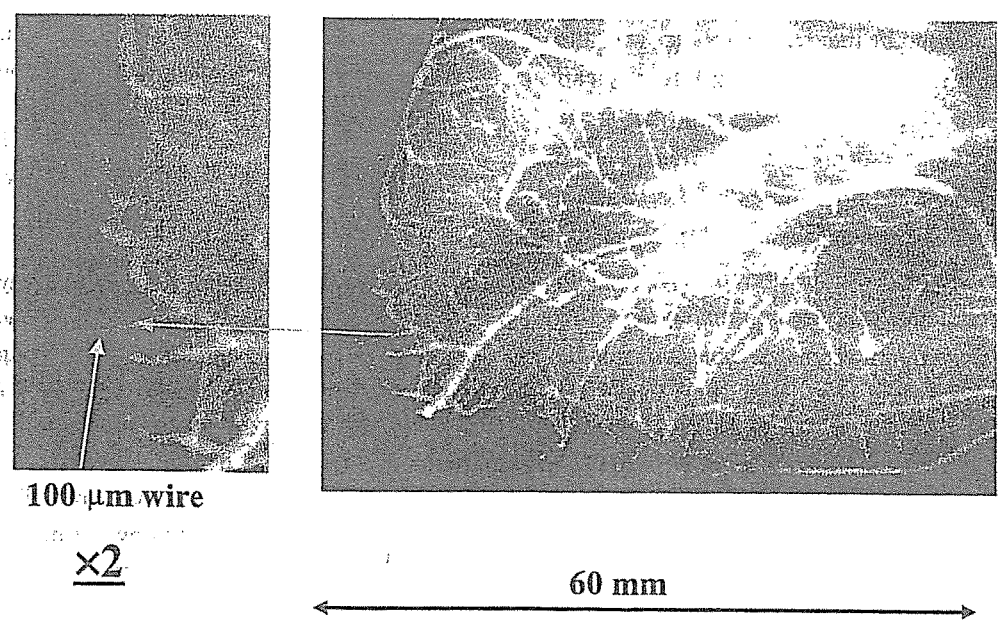

Fig. 10. Angiogram of extracted dog heart using iodine microspheres with tube voltage of 60 kV.

Fig. 11. Angiogram of rabbit thigh with tube voltage of 60 kV.

5. DISCUSSION AND CONCLUSIONS

In summary, we employed an x-ray generator with a cerium-target tube and succeeded in producing cerium characteristic x rays, which can be absorbed easily by iodine-based contrast mediums. The characteristic x-ray intensities increased with increases in the tube voltage, and bremsstrahlung rays were absorbed effectively by the filter.

Although the cerium x-ray generator used in this research produces both the characteristic and the bremsstrahlung x rays, bremsstrahlung intensity can be decreased effectively by considering the angle dependence without using the filter, since bremsstrahlung rays are not emitted in the opposite direction to that of electron acceleration. Subsequently, the generator produced maximum number of characteristic photons was approximately 3×10^7 photons/cm^2 • s at 1.0 m from the source, and the photon count rate can be increased easily by improving the target.

ACKNOWLEDGMENT

This work was supported by Grants-in-Aid for Scientific Research (13470154, 13877114, and 16591222) and Advanced Medical Scientific Research from MECSST, Health and Labor Sciences Research Grants (RAMT-nano-001, RHGTEFB-genome-005 and RHGTEFB-saisei-003), Grants from Keiryo Research Foundation, The Promotion and Mutual Aid Corporation for Private Schools of Japan, Japan Science and Technology Agency (JST), and New Energy and Industrial Technology Development Organization (NEDO, Industrial Technology Research Grant Program in '03).

REFERENCES

1) Thompson A C, Zeman H D, Brown G S, Morrison J, Reiser P, Padmanabahn V, Ong L, Green S, Giacomini J, Gordon H and Rubenstei E: First operation of the medical research facility at the NSLS for coronary angiography. *Rev. Sci. Instrum.*, 63:625-628, 1992.

2) Mori H, Hyodo K, Tanaka E, Mohammed M, Yamakawa A, Shinozaki Y, Nakazawa H, Tanaka Y, Sekka T, Iwata Y, Honda S, Umetani K, Ueki H, Yokoyama T, Tanioka K, Kubota M, Hosaka H, Ishizawa N and Ando M: Small-vessel radiography in situ with monochromatic synchrotoron radiation. *Radiology*, 201:173-177, 1996.

3) Hyodo K, Ando M, Oku Y, Yamamoto S, Takeda T, Itai Y, Ohtsuka S, Sugishita Y and Tada J: Development of a two-dimensional imaging system for clinical applications of intravenous coronary angiography using intense synchrotron radiation produced by a multipole wiggler. *J. Synchrotron Rad.*, 5:1123-1126, 1998.

4) Davis T J, Gao D, Gureyev T E, Stevenson A W and Wilkims S W: Phase-contrast imagimg of weakly absorbing materials using hard x-rays. *Nature*, 373:595-597, 1995.

5) Momose A, Takeda T, Itai Y and Hirano K: Phase-contrast x-ray computed tomography for observing biological soft tissues. *Nature Medicine*, 2:473-475, 1996.

6) Ando M, Maksimenko A, Sugiyama H, Pattanasiriwisawa W, Hyodo K and Uyama C: A simple x-ray dark- and bright- field imaging using achromatic Laue optics. *Jpn. J. Appl. Phys.*, 41: L1016-L1018, 2002.

7) Sato E, Kimura S, Kawasaki S, Isobe H, Takahashi K, Tamakawa Y and Yanagisawa T: Repetitive flash x-ray generator utilizing a simple diode with a new type of energy-selective function. *Rev. Sci. Instrum.*, 61:2343-2348, 1990.

8) Sato E, Sagae M, Takahashi K, Oizumi T, Ojima

H, Takayama K, Tamakawa Y, Yanagisawa T, Fujiwara A and Mitoya K: High-speed soft x-ray generators in biomedicine. *SPIE*, 2513:649-667, 1994.

9) Sato E, Sagae M, Takahashi K, Shikoda A, Oizumi T, Ojima H, Takayama K, Tamakawa Y, Yanagisawa T, Fujiwara A and Mitoya K: Dual energy flash x-ray generator, *SPIE*, 2513:723-735, 1994.

10) Shikoda A, Sato E, Sagae M, Oizumi T, Tamakawa Y and Yanagisawa T: Repetitive flash x-ray generator having a high-durability diode driven by a two-cable-type line pulser. *Rev. Sci. Instrum.*, 65: 850-856, 1994.

11) Sato E, Takahashi K, Sagae M, Kimura S, Oizumi T, Hayasi Y, Tamakawa Y and Yanagisawa T: Sub-kilohertz flash x-ray generator utilizing a glass-enclosed cold-cathode triode. *Med. & Biol. Eng. & Comput.*, 32:289-294, 1994.

12) Takahashi K, Sato E, Sagae M, Oizumi T, Tamakawa Y and Yanagisawa T: Fundamental study on a long-duration flash x-ray generator with a surface-discharge triode. *Jpn. J. Appl. Phys.*, 33: 4146-4151, 1994.

13) Sato E, Sagae M, Shikoda A, Takahashi K, Oizumi T, Yamamoto M, Takabe A, Sakamaki K, Hayasi Y, Ojima H, Takayama K and Tamakawa Y: High-speed soft x-ray techniques, *SPIE*, 2869: 937-955, 1996.

14) Sato E, Hayasi Y, Tanaka E, Mori H, Kawai T, Usuki T, Sato K, Obara H, Ichimaru T, Takayama K, Ido H and Tamakawa Y: Quasi-monochromatic radiography using a high-intensity quasi-x-ray laser generator. *SPIE*, 4682:538-548, 2002.

15) Sato E, Hayasi Y, Germer R, Tanaka E, Mori H, Kawai T, Obara H, Ichimaru T, Takayama K and Ido H: Intense characteristic x-ray irradiation from weakly ionized linear plasma and applications. *Jpn. J. Med. Imag. Inform. Sci.*, 20:148-155. 2003.

16) Sato E, Hayasi Y, Germer R, Tanaka E, Mori H, Kawai T, Obara H, Ichimaru T, Takayama K and Ido H: Irradiation of intense characteristic x-rays from weakly ionized linear molybdenum plasma. *Jpn. J. Med. Phys.*, 23:123-131, 2003.

17) Sato E, Hayasi Y, Germer R, Tanaka E, Mori H, Kawai T, Ichimaru T, Takayama K and Ido H: Quasi-monochromatic flash x-ray generator utilizing weakly ionized linear copper plasma. *Rev. Sci. Instrum.*, 74:5236-5240, 2003.

18) Sato E, Hayasi Y, Germer R, Tanaka E, Mori H, Kawai T, Ichimaru T, Sato S, Takayama K and Ido H: Sharp characteristic x-ray irradiation from weakly ionized linear plasma. *J. Electron Spectrosc. Related Phenom.*, 137-140:713-720, 2004.

19) Sato E, Germer R, Hayasi Y, Murakami K, Koorikawa Y, Tanaka E, Mori H, Kawai T, Ichimaru T, Obata F, Takahashi K, Sato S, Takayama K and Ido H: Weakly ionized cerium plasma radiography. *SPIE*, 5210:12-21, 2003.

20) Sato E, Tanaka E, Mori H, Kawai T, Ichimaru T, Sato S, Takayama K and Ido H: Demonstration of enhanced K-edge angiography using a cerium target x-ray generator. *Med. Phys.*, 31: 3017-3022, 2004.

21) Sato E, Sato K and Tamakawa Y: Film-less computed radiography system for high-speed Imaging. *Ann. Rep. Iwate Med. Univ. Sch. Lib. Arts and Sci.*, 35:13-23, 2000.

セリウムX線装置と酸化セリウムフィルターを利用したコーンビームKエッジ造影
——微小血管の観察——

市丸俊夫[*1] 山寺 亮[*1] 佐藤英一[*2]
田中越郎[*3] 盛 英三[*4] 河合敏明[*5]
佐藤成大[*6] 高山和喜[*7]

(2004年10月30日受付, 2005年1月13日受理)

要旨：セリウム対陰極から発生するK系列特性X線はヨウ素系造影剤に効率良く吸収されるので，コーンビームによるKエッジ造影に有用である。X線装置はメインコントローラー，そして高電圧回路とX線管のユニットなどからなる。X線管はガラス封じ込み二極管で，セリウム対陰極と0.5 mm厚のベリリウム窓を有する。管電圧と電流の最大値はそれぞれ65 kVと0.4 mAで，実効焦点サイズは1.3×0.9 mmであった。セリウムのK系列特性X線は酸化セリウムのフィルターを用いて制動X線を吸収することにより得られ，X線強度は線源から1.0 mの位置で，管電圧60 kV，そして管電流0.4 mAの条件下で，0.5 μC/kg•sであった。血管には直径15 μmのヨウ素プラスチック微小球が充填され，デジタル撮影装置（CR）で造影された。動物ファントムの造影では，100 μm程度の血管が高コントラストで観察できた。

キーワード：X線発生装置，セリウムターゲット，準単色X線，特性X線，Kエッジ造影

*1弘前大学医学部保健学科放射線技術科学専攻
〒036-8565 青森県弘前市本町66番地1
*2岩手医科大学教養部物理学科
〒020-0015 岩手県盛岡市本町通3-16-1
*3東京農業大学応用生物科学部栄養科学科
〒020-0015 東京都世田谷区桜ヶ丘1-1-1
*4国立循環器センター研究所心臓生理部
〒565-8565 大阪府吹田市藤白台5-7-1
*5浜松ホトニクス電子管事業部
〒438-0193 静岡県磐田郡豊岡村下神増314-5
*6岩手医科大学医学部細菌学講座
〒020-0015 岩手県盛岡市内丸19-1
*7東北大学流体力学研究所
〒980-8577 宮城県仙台市青葉区片平2-1-1

Circ J 2005; **69:** 1315–1319

Angiotensin-Converting Enzyme Genotype is Not Associated With Exercise Capacity or the Training Effect of Cardiac Rehabilitation in Patients After Acute Myocardial Infarction

Yoshitaka Iwanaga, MD; Isao Nishi, MD; Koh Ono, MD; Shuichi Takagi, MD; Yoshiaki Tsutsumi, MD; Masanori Ozaki, MD; Teruo Noguchi, MD; Hiroshi Takaki, MD; Naoharu Iwai, MD; Hiroshi Nonogi, MD; Yoichi Goto, MD

Background The relationship of the genotype for the angiotensin-converting enzyme (ACE) with exercise capacity or training effects has been studied in athletes or healthy persons, but recently the ACE DD genotype was reported to be associated with decreased exercise capacity in patients with congestive heart failure. Therefore, in the present study the association between the ACE genotype and exercise capacity was investigated in patients with acute myocardial infarction (AMI) participating in cardiac rehabilitation (CR) for 3 months.

Methods and Results The study population comprised 168 patients stratified as II (n=75), ID (n=67), and DD (n=26) according to ACE genotype. Baseline left ventricular ejection fraction (LVEF) was similar among the genotype groups. In all patients, exercise capacity (peak work rate (PWR) and peak oxygen uptake ($P\dot{V}O_2$)) significantly increased after CR. However, no differences were observed in PWR and $P\dot{V}O_2$ among the genotype groups at baseline or after CR. The results were similar even when analyzed in 60 patients with left ventricular (LV) dysfunction (LVEF <45%).

Conclusion The present study suggests that there is no association between ACE I/D polymorphism and exercise capacity in patients after AMI, even with LV dysfunction. Furthermore, ACE genotype may have no influence on the effects of CR after AMI. (*Circ J* 2005; **69:** 1315–1319)

Key Words: ACE genotype; Cardiac rehabilitation; Left ventricular dysfunction; Myocardial infarction

Exercise-based cardiac rehabilitation (CR) improves functional capacity and reduces mortality in patients with acute myocardial infarction (AMI).[1–3] Although the exact mechanisms by which exercise reduces mortality are unclear, one of the definite effects is improving exercise tolerance.[4,5] Exercise tolerance itself is a multifactorial phenotype influenced by several genetic and environmental factors and the training benefits may be attributed predominantly to adaptations in the peripheral circulation and skeletal muscles rather than to adaptations in cardiac performance.[6] However, the precise mechanism is not fully understood.

Over the past decade, the insertion/deletion (I/D) polymorphism of a 287-bpAlu element in intron 16 of the angiotensin-converting enzyme (ACE) gene has been extensively investigated in a spectrum of cardiovascular phenotypes, because of its correlation with serum ACE activity.[7] Many of the previous studies have shown a positive association between the DD genotype and an increased risk of MI, and recent reports suggested a potential pharmacogenetic interaction between the ACE genotype and therapy with β-blockers in chronic heart failure (CHF) patients.[8] However, results in hypertension, left ventricular (LV) hypertrophy, cardiomyopathy and restenosis after percutaneous transluminal coronary angioplasty remain quite controversial.

Several studies have shown that the ACE I allele is associated with enhanced physical performance. An increased frequency of the ACE I allele has been reported in army recruits, rowers, and high altitude mountaineers.[9,10] The ACE I allele has been associated with higher peak oxygen consumption ($P\dot{V}O_2$) levels in postmenopausal women.[11] Moreover, a recent study has demonstrated an association of the ACE DD genotype with decreased exercise tolerance in 57 patients with CHF.[12] However, the association between ACE genotype and exercise capacity or the effect of exercise training in patients after AMI with or without LV dysfunction remains unknown. Accordingly, in the current study, we examined exercise capacity in relation to ACE polymorphism in patients with AMI participating in CR for 3 months.

Methods

Study Population

One hundred sixty-eight consecutive patients who were admitted to the National Cardiovascular Center with a diagnosis of AMI and participated in the 3-month CR program with exercise training between January 2001 and September 2002 were recruited. The CR program started approximately 2 weeks after the onset of AMI and continued for 3 months. Patients exercised for 60 min 4–5 times a

(Received June 27, 2005; revised manuscript received August 9, 2005; accepted August 30, 2005)
National Cardiovascular Center, Suita, Japan
Mailing address: Yoichi Goto, MD, Division of Cardiology, National Cardiovascular Center, 5-7-1 Fujishirodai, Suita 565-8565, Japan. E-mail: ygoto@hsp.ncvc.go.jp

Table 1 Characteristics of the Patients With AMI According to Their ACE Genotype

	II	ID	DD	p value
N	75	67	26	
F, %	14	14	19	0.851
Age, years	59±1	56±1	60±2	0.139
BW, kg	61.3±1.2	65.4±1.4	61.7±2.1	0.068
BMI, kg/m²	23.1±0.4	24.1±0.4	23.0±0.6	0.160
DM, %	55	40	59	0.102
HLP, %	60	61	59	0.970
HT, %	61	54	50	0.540
Smoking, %	64	63	81	0.164
LVEF, %	45±1	48±1	47±2	0.129
Heart rate, beats/min	72±2	76±2	74±3	0.336
ACE inhibitor, %	58	51	59	0.679
β-blocker, %	32	27	11	0.078

AMI, acute myocardial infarction; BW, body weight; BMI, body mass index; DM, diabetes mellitus; HLP, hyperlipidemia; HT, hypertension; LVEF, left ventricular ejection fraction; ACE, angiotensin converting enzyme. Values are mean±SE.

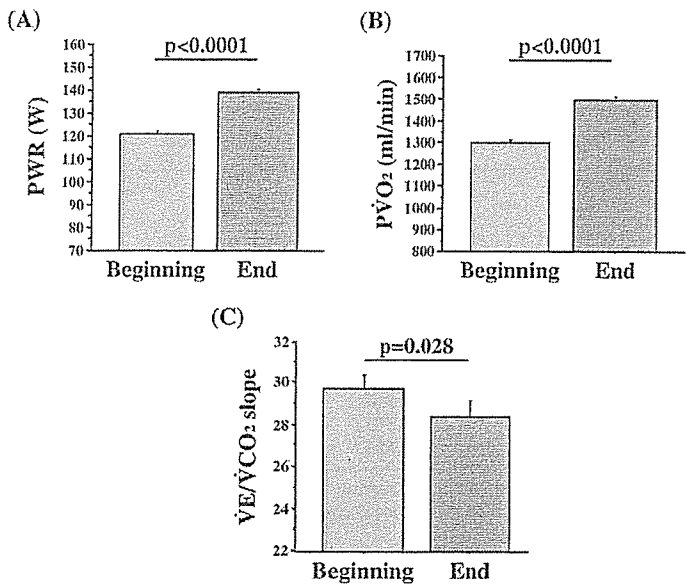

Fig 1. Changes in the cardiopulmonary exercise parameters after 3-month cardiac rehabilitation in 168 patients. (A) peak work rate (PWR), (B) peak oxygen consumption (PV̇O₂), and (C) the slope of minute ventilation–carbon dioxide production relationship (V̇E/V̇CO₂ slope). Bars represent mean±SE.

week: 2–3 times in hospital under supervision and the remaining 2–3 times at home. Exercise consisted of aerobic dance and stationary bicycle riding in hospital and brisk walking at home. The training heart rate (HR) was determined according to the HR reserve method or Karvonen's equation (k=0.5–0.6): training HR=(peak HR−rest HR)×k+rest HR, where peak and rest HR were obtained in a symptom-limited exercise test at the beginning of the program.[13] Six patients failed to complete the 3-month CR program and so the total number of subjects was 162.

Cardiopulmonary Exercise Testing (CPX)

All patients underwent symptom-limited incremental CPX on a bicycle ergometer at the beginning and end of the 3-month CR program. Breath-by-breath respiratory gas exchange measurements were performed using a computerized metabolic cart (Minato Products, Japan). Details of the test protocol have been published elsewhere![14]

Assessment of LV Systolic Function

LV ejection fraction (LVEF) was determined as an index of LV systolic function by contrast left ventriculography at the beginning of the CR program (approximately 3 weeks after AMI onset). LVEF <45% was considered as LV dysfunction.

Blood Tests

Genomic DNA was isolated from peripheral leukocytes as previously reported![15] The ACE genotypes were determined by polymerase chain reaction as previously reported![15]

The institutional ethics committee approved the study and written informed consent was obtained from each patient before participation.

Statistics

The ANOVA method was used to assess the statistical significance of differences in means across genotype groups. All data are expressed as the mean value±SD. A p-value <0.05 was considered significant. All statistical analyses were performed with the JMP statistical package (SAS Institute Inc, Cary, NC, USA).

Results

Patient Characteristics

The 168 patients were divided into 3 groups according to

Table 2 Exercise Capacity at the Beginning and End of Cardiac Rehabilitation of the Patients With AMI According to Their ACE Genotype

	II (n=74)	ID (n=62)	DD (n=26)	p value
Beginning				
PWR	118±3	125±4	119±6	0.285
$P\dot{V}O_2$	1,262±42	1,370±46	1,292±71	0.218
$\dot{V}E/\dot{V}CO_2$	30.1±0.9	27.9±1.1	30.1±1.6	0.243
End				
PWR	136±4	141±4	133±6	0.452
$P\dot{V}O_2$	1,465±49	1,562±53	1,414±82	0.229
$\dot{V}E/\dot{V}CO_2$	27.7±0.7	27.5±0.8	27.8±1.2	0.960
Increase rate				
%PWR	13.6±1.5	12.9±1.6	12.0±2.5	0.863
$\%P\dot{V}O_2$	14.5±1.9	14.3±2.0	10.4±3.2	0.507
$\%\dot{V}E/\dot{V}CO_2$	−4.4±2.4	−1.7±2.8	−5.1±4.3	0.704

AMI, acute myocardial infarction; ACE, angiotensin converting enzyme; PWR, peak work rate; $P\dot{V}O_2$, peak oxygen consumption; $\dot{V}E/\dot{V}CO_2$, minute ventilation carbon dioxide production relationship. Values are mean±SE.

Table 3 Exercise Capacity at the Beginning and End of Cardiac Rehabilitation of the Patients With AMI and LV Dysfunction (LVEF <45%) According to Their ACE Genotype

	II (n=31)	ID (n=21)	DD (n=8)	p value
Beginning				
PWR	113±5	124±6	105±10	0.192
$P\dot{V}O_2$	1,210±60	1,331±73	1,123±119	0.259
$\dot{V}E/\dot{V}CO_2$	30.9±1.2	28.3±1.7	28.7±3.2	0.428
End				
PWR	127±6	136±7	114±11	0.225
$P\dot{V}O_2$	1,354±73	1,501±90	1,202±141	0.170
$\dot{V}E/\dot{V}CO_2$	29.9±1.1	27.4±1.4	25.8±2.4	0.228
Increase rate				
%PWR	7.7±1.9	11.2±2.3	9.2±3.5	0.509
$\%P\dot{V}O_2$	8.5±3.1	12.4±3.7	7.8±5.8	0.681
$\%\dot{V}E/\dot{V}CO_2$	2.0±3.6	0.1±4.8	−10.1±8.8	0.453

AMI, acute myocardial infarction; LV, left ventricular; LVEF, LV ejection fraction; ACE, angiotensin converting enzyme; PWR, peak work rate; $P\dot{V}O_2$, peak oxygen consumption; $\dot{V}E/\dot{V}CO_2$, minute ventilation carbon dioxide production relationship. Values are mean±SE.

their ACE genotype, the frequencies of which were in a Hardy-Weinberg equilibrium in this population. Baseline characteristics of the 3 groups are summarized in Table 1. Sex, mean age, body weight, body mass index and risk factors did not differ significantly among the genotypes. No significant difference in either resting LVEF or HR was detected. Although the subjects with the DD genotype had a trend toward a lower percentage of β-blocker treatment, no significant difference was observed.

Effects of CR on Exercise Capacity

Fig 1 shows the effects of 3-month CR on the CPX parameters in all subjects. The peak work rate (PWR), $P\dot{V}O_2$ and the slope of the minute ventilation–carbon dioxide production relationship ($\dot{V}E/\dot{V}CO_2$ slope) improved significantly after 3 months of CR (12.1%, 13.3%, −3.9% from baseline, respectively).

Exercise Capacity and Effects According to ACE Genotype

Table 2 shows the CPX data at the beginning and end of the 3-month CR stratified by the ACE genotype. It also shows the increase rate ((end−beginning)/beginning×100; %). No significant differences in PWR, $P\dot{V}O_2$ or $\dot{V}E/\dot{V}CO_2$ slope were observed among the 3 genotype groups at either time point. All parameters improved by a similar magnitude across the genotypes after 3-month CR as demonstrated by the increase rate.

Subanalysis was performed in patients with LV dysfunction (LVEF <45%, n=60), which is shown in Table 3. The pattern of the genotype distributions did not differ significantly between the patients with or without LV dysfunction (chi-square test, p=0.269). No significant differences in the 3 exercise parameters were observed among the 3 genotype groups at either the beginning or the end. Also, there were no significant differences in the increase rate of the 3 parameters among the 3 groups. Similar results were obtained in the subanalysis of male patients (63II/54ID/22DD) (data not shown).

Discussion

In the present study, based upon the hypothesis that the ACE genotype may have an association with the exercise capacity, we investigated this association in patients with AMI participating in CR for 3 months. However, we found no association between ACE I/D polymorphism and exercise capacity in this patient group, even in those with LV dysfunction. Furthermore, the ACE genotype may have no influence on the training effects of CR after AMI. Although many studies have explored the relationship of ACE geno-